J Math Chem (2011) 49:1573–1586
DOI 10.1007/s10910-011-9844-1

ORIGINAL PAPER

Modelling synergistic action of laccase-based biosensor utilizing simultaneous substrates conversion

Evelina Gaidamauskaitė · Romas Baronas · Juozas Kulys

Received: 15 October 2010 / Accepted: 10 May 2011 / Published online: 21 May 2011

Abstract The response of a laccase-based amperometric biosensor that acts in a synergistic manner was modelled digitally. A mathematical model of the biosensor is based on a system of non-linear reaction diffusion equations. The modelling biosensor comprises three compartments, an enzyme layer, a dialysis membrane and an outer diffusion layer. By changing input parameters the biosensor action was analysed with a special emphasis to the influence of the species concentrations on the synergy of the simultaneous substrates conversion. The digital simulation was carried out using the finite difference technique.

Keywords Mathematical modelling · Simulation · Biosensor · Laccase · Synergistic scheme

1 Introduction

Biosensors are analytical devices made up of a combination of a biological entity, usually an enzyme, that recognizes a specific analyte and the transducer that translates the biorecognition event into a signal [1,2]. The signal is usually proportional to the concentration of the target analyte. Amperometric biosensors measure the changes in the output current arising on the electrode because of the direct electrochemical reduction or oxidation of the biochemical reaction product [3]. Amperometric biosensors

E. Gaidamauskaitė (✉) · R. Baronas
Faculty of Mathematics and Informatics, Vilnius University, Naugarduko 24, 03225 Vilnius, Lithuania
e-mail: evelina.gaidamauskaite@mif.vu.lt

J. Kulys
Department of Chemistry and Bioengineering, Vilnius Gediminas Technical University, Sauletekio Ave. 11, 10223 Vilnius, Lithuania
e-mail: juozas.kulys@vgtu.lt

are known to be relatively cheap, sensitive and reliable devices, widely used in clinical diagnostics, drug discovery, food analysis and environment monitoring and some other purposes [4–7].

There are many different schemes of enzymatic catalysis apart from the simplest Michaelis-Menten case that might be exploited for the bioelectrocatalysis and the construction of biosensors [8,9]. Synergistic scheme of substrates conversion is of particular interest due to the fact that this scheme allows producing highly sensitive bioelectrodes and powerful biofuel cells [10–14]. In the synergistic scheme, an enzyme catalyses the parallel conversion of substrates into the products, with the concomitant cross-reaction of the substrates and the products. Moreover, in this case, the average rate of substrates conversion exceeds the rate of individual reaction steps [15–17].

A number of characteristics are important in the development of actual biosensors [1,2,4,9]. To improve the productivity as well as the efficiency of the biosensor design, a model of the biosensor should be built [18,19]. Mathematical models have been widely used to study and optimise analytical characteristics of the biosensors [20–24].

Recently, the laccase-based bioelectrode utilising synergistic N-substituted phenothiazines and phenoxazines oxidation in the presence of hexacyanoferrate(II) was built and investigated [25]. The synergistic process was analytically investigated assuming the steady state conditions, ignoring the mass transport and applying many other simplifications. The action of bioelectrodes includes not only biocatalytical conversion but also the mass transport of substrates as well as products [1,2,4,26]. The diffusion limitations causes bioelectrode sensitivity changes. For the accurate prediction of the bioelectrode response, the mass transport by diffusion has to be considered together with the biocatalytical conversion [27–29]. The modelling of these processes by an analytical solution of the system of differential equations is practically impossible [30,31].

This paper presents a mathematical model of a laccase-based biosensor utilizing simultaneous substrates conversion. The developed model is based on non-stationary non-linear reaction-diffusion equations [24,30]. The modelling biosensor comprises three compartments, an enzyme layer, a dialysis membrane and an outer diffusion layer. By changing input parameters the biosensor action was analysed with a special emphasis to the influence of the species concentrations on the synergy of the simultaneous substrates conversion. The digital simulation was carried out using the finite difference technique [24,30,32].

2 Modelling biosensor

In this paper a laccase-based biosensor is modelled [25]. We assume that it is composed of a graphite electrode covered with the net (mesh = 160, thickness of the thread 100 μm) and the enzyme solution. The enzyme layer is separated from the bulk solution by means of the dialysis membrane. The diffusion layer where the flux of the substances takes place is also considered. The schematic view of the modelled biosensor is presented in the Fig. 1.

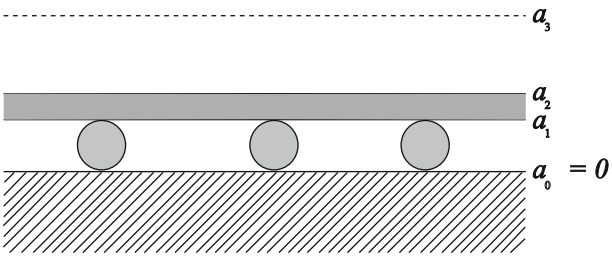

Fig. 1 The schematic view of the laccase-based amperometric biosensor

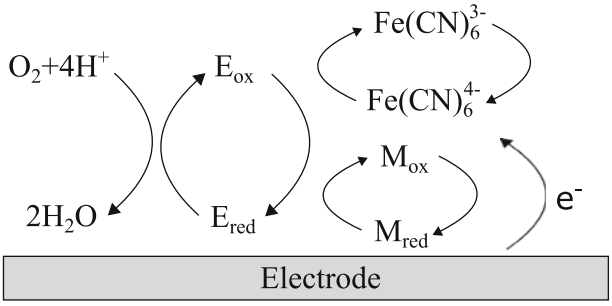

Fig. 2 Scheme of electron transfer in laccase biosensor

The scheme of the laccase action comprises the stadium of oxidized laccase interaction with two substrates as well as a cross reaction of the oxidized mediator and ferrocyanide [25]. The laccase is activated with oxygen,

$$\text{Laccase(red)} + \text{O} + 4\text{H}^+ \xrightarrow{k_1} \text{Laccase(ox)} + 2\text{H}_2\text{O}, \tag{1}$$

$$\text{Laccase(ox)} + 4\text{Fe(CN)}_6^{4-} \xrightarrow{k_2} \text{Laccase(red)} + 4\text{Fe(CN)}_6^{3-}, \tag{2}$$

$$\text{Laccase(ox)} + 4\text{M}_{red} \xrightarrow{k_3} \text{Laccase(red)} + 4\text{M}_{ox}, \tag{3}$$

$$\text{M}_{ox} + \text{Fe(CN)}_6^{4-} \xrightarrow{k_4} \text{M}_{red} + \text{Fe(CN)}_6^{3-}, \tag{4}$$

where Laccase(red) and Laccase(ox) are the reduced and oxidized forms of laccase, O - oxygen (O_2), H_2O - water, H^+ stands for the hydrogen ion, $Fe(CN)_6^{4-}$ is the hexacyanoferrate(II) (ferrocyanide), $Fe(CN)_6^{3-}$ is the hexacyanoferrate(III) (ferricyanide), M_{red}, M_{ox}—stand for the reduced and oxidized mediators respectively, k_1, k_2, k_3, k_4 are the reaction rate constants (see Fig. 2).

On the electrode surface the ferricyanide is reduced to ferrocyanide whereas oxidized mediator is converted to its reduced form,

$$\text{Fe(CN)}_6^{3-} + e^- \longrightarrow \text{Fe(CN)}_6^{4-}, \tag{5}$$

$$\text{M}_{ox} + e^- \longrightarrow \text{M}_{red}. \tag{6}$$

In the terms of substrates and products the reaction scheme (1)–(6) can be written as follows:

$$E_{red} + \mathrm{O} + 4\mathrm{H}^{+} \xrightarrow{k_1} E_{ox} + 2\mathrm{H_2O}, \tag{7}$$

$$E_{ox} + 4S_1 \xrightarrow{k_2} E_{red} + 4P_1, \tag{8}$$

$$E_{ox} + 4S_2 \xrightarrow{k_3} E_{red} + 4P_2, \tag{9}$$

$$P_2 + S_1 \xrightarrow{k_4} S_2 + P_1, \tag{10}$$

$$P_1 + e^{-} \longrightarrow S_1, \tag{11}$$

$$P_2 + e^{-} \longrightarrow S_2, \tag{12}$$

where E_{red} and E_{ox} correspond to the reduced and the oxidized laccase enzyme, respectively, S_1 and S_2 are the substrates, P_1, P_2—stand for the products of the reactions. S_2 and P_2 are called the reduced and the oxidized mediators, respectively. The products P_1 and P_2 are the electrochemically active substances.

3 Mathematical model

The biosensor model involves the following regions: an enzyme-loaded nylon net, a dialysis membrane, an outer diffusion limiting region, and a convective region where the analyte concentration is maintained constant. Due to the relatively small volume of the nylon net in comparison with the volume of the enzyme, the enzyme-loaded mesh can be assumed as a periodic media, and the homogenisation process can be applied to the enzyme-loaded mesh [33]. These assumptions lead to a three compartment model. The homogenised enzyme layer corresponds to the first compartment. The dialysis membrane and the outer diffusion are the next two compartments.

3.1 Governing equations

Assuming the homogeneous distribution of immobilised enzyme, the mass transport and the reaction kinetics in the enzyme layer of the uniform thickness can be described by the following system of the reaction-diffusion equations ($0 < x < a_1,\ t > 0$):

$$\frac{\partial E_{red,1}}{\partial t} = D_{E_{red,1}} \frac{\partial^2 E_{red,1}}{\partial x^2} + 4k_2 E_{ox,1} S_{1,1} - k_1 E_{red,1} O_1 + 4k_3 E_{ox,1} S_{2,1}, \tag{13a}$$

$$\frac{\partial E_{ox,1}}{\partial t} = D_{E_{ox,1}} \frac{\partial^2 E_{ox,1}}{\partial x^2} + k_1 E_{red,1} O_1 - 4k_2 E_{ox,1} S_{1,1} - 4k_3 E_{ox,1} S_{2,1}, \tag{13b}$$

$$\frac{\partial S_{1,1}}{\partial t} = D_{S_{1,1}} \frac{\partial^2 S_{1,1}}{\partial x^2} - 4k_2 E_{ox,1} S_{1,1} - k_4 P_{2,1} S_{1,1}, \tag{13c}$$

$$\frac{\partial S_{2,1}}{\partial t} = D_{S_{2,1}} \frac{\partial^2 S_{2,1}}{\partial x^2} - 4k_3 E_{ox,1} S_{2,1} + k_4 P_{2,1} S_{1,1}, \tag{13d}$$

$$\frac{\partial P_{1,1}}{\partial t} = D_{P_{1,1}} \frac{\partial^2 P_{1,1}}{\partial x^2} + 4k_2 E_{ox,1} S_{1,1} + k_4 P_{2,1} S_{1,1}, \tag{13e}$$

$$\frac{\partial P_{2,1}}{\partial t} = D_{P_{2,1}} \frac{\partial^2 P_{2,1}}{\partial x^2} + 4k_3 E_{ox,1} S_{2,1} - k_4 P_{2,1} S_{1,1}, \tag{13f}$$

$$\frac{\partial O_1}{\partial t} = D_{O_1} \frac{\partial^2 O_1}{\partial x^2} - k_1 E_{red,1} O_1, \tag{13g}$$

where $E_{red,1}$, $E_{ox,1}$, $S_{i,1}$, $P_{i,1}$ and O_1 stand for the concentrations of the reduced and oxidized forms of the enzyme, ith substrate, ith product and oxygen, respectively, a_1 is the thickness of the enzyme layer, $D_{E_{red,1}}$, $D_{E_{ox,1}}$, $D_{S_{i,1}}$, $D_{P_{i,1}}$ and D_{O_1} are the diffusion coefficients, $i = 1, 2$.

In the dialysis membrane as well as in the outer diffusion layer no enzymatic reaction occurs. Hence, only the mass transport by diffusion and the electrochemical reaction (11) are modelled ($a_{j-1} < x < a_j,\ t > 0$),

$$\frac{\partial S_{1,j}}{\partial t} = D_{S_{1,j}} \frac{\partial^2 S_{1,j}}{\partial x^2} - k_4 P_{2,j} S_{1,j}, \tag{14a}$$

$$\frac{\partial S_{2,j}}{\partial t} = D_{S_{2,j}} \frac{\partial^2 S_{2,j}}{\partial x^2} + k_4 P_{2,j} S_{1,j}, \tag{14b}$$

$$\frac{\partial P_{1,j}}{\partial t} = D_{P_{1,j}} \frac{\partial^2 P_{1,j}}{\partial x^2} + k_4 P_{2,j} S_{1,j}, \tag{14c}$$

$$\frac{\partial P_{2,j}}{\partial t} = D_{P_{2,j}} \frac{\partial^2 P_{2,j}}{\partial x^2} - k_4 P_{2,j} S_{1,j}, \tag{14d}$$

$$\frac{\partial O_j}{\partial t} = D_{O_j} \frac{\partial^2 O_j}{\partial x^2}, \tag{14e}$$

where $S_{i,j}$, $P_{i,j}$ and O_j stand for the concentrations of the ith substrate, ith product and oxygen in the dialysis membrane ($j = 2$) and the diffusion layer ($j = 3$), respectively, a_1 is the thickness of the enzyme layer, $a_2 - a_1$ and $a_3 - a_2$ are the thicknesses of the membrane and the diffusion layer, respectively, $D_{S_{i,j}}$, $D_{P_{i,j}}$ and D_{O_j} are the diffusion coefficients, $i = 1, 2$, $j = 2, 3$.

3.2 Initial conditions

The biosensor operation starts when the substrates appear on the boundary of the diffusion layer ($t = 0$),

$$S_{i,j} = 0, \quad x \in [a_{j-1}, a_j], \quad j = 1, 2, \tag{15a}$$

$$S_{i,3} = 0, \quad x \in [a_2, a_3), \tag{15b}$$

$$S_{i,3} = S_{i,0}, \quad x = a_3, \tag{15c}$$

where $S_{i,0}$ is the concentration of the ith substrate in the buffer solution, $a_0 = 0$, $i = 1, 2$.

Initially, the oxygen is assumed to be of uniform concentration, while the products are assumed of zero concentration ($t = 0$),

$$P_{i,j} = 0, \quad O_j = O_0, \quad x \in [a_{j-1}, a_j], \quad j = 1, 2, 3, \tag{16}$$

where O_0 is the initial concentration of the oxygen.

The whole enzyme is initially in the reduced form ($t = 0$),

$$E_{red,1} + E_{ox,1} = E_0, \quad E_{red,1} = E_0, \quad E_{ox,1} = 0, \quad x \in [0, a_1], \tag{17}$$

where E_0 stands for the initial as well as the total concentration of the enzyme.

3.3 Boundary conditions

On the electrode surface the products are consumed and the substrates are regenerated by reactions (11) and (12) ($t > 0$),

$$P_{i,1} = 0, \quad x = 0, \tag{18a}$$

$$D_{S_{i,1}} \left.\frac{\partial S_{i,1}}{\partial x}\right|_{x=0} = -D_{P_{i,1}} \left.\frac{\partial P_{i,1}}{\partial x}\right|_{x=0}, \quad i = 1, 2. \tag{18b}$$

Assuming the impenetrable plate surface, the mass flux of the electro-inactive substance vanishes at this boundary ($t > 0$),

$$\left.\frac{\partial O_1}{\partial x}\right|_{x=0} = 0. \tag{19}$$

During the biosensor operation the enzyme remains locked in the enzyme layer ($t > 0$),

$$\left.\frac{\partial E_{ox}}{\partial x}\right|_{x=0} = \left.\frac{\partial E_{ox}}{\partial x}\right|_{x=a_1} = \left.\frac{\partial E_{red}}{\partial x}\right|_{x=0} = \left.\frac{\partial E_{red}}{\partial x}\right|_{x=a_1} = 0. \tag{20}$$

The outer diffusion layer ($a_2 < x < a_3$) can be treated as the Nernst diffusion layer [30]. According to the Nernst approach the layer of the thickness ($a_3 - a_2$) remains constant. In the bulk solution the concentrations of the substances remain constant ($t > 0$),

$$S_{1,3} = S_{1,0}, \quad S_{2,3} = S_{2,0}, \quad P_{1,3} = 0, \quad P_{2,3} = 0, \quad O_3 = O_0, \quad x = a_3. \tag{21}$$

On the boundary between the adjacent regions having different diffusivities, we define the matching conditions ($t > 0$),

$$D_{S_{i,j}} \frac{\partial S_{i,j}}{\partial x}\bigg|_{x=a_j} = D_{S_{i,j+1}} \frac{\partial S_{i,j+1}}{\partial x}\bigg|_{x=a_j}, \quad S_{i,j} = S_{i,j+1}, \quad x = a_j, \tag{22a}$$

$$D_{P_{i,j}} \frac{\partial P_{i,j}}{\partial x}\bigg|_{x=a_j} = D_{P_{i,j+1}} \frac{\partial P_{i,j+1}}{\partial x}\bigg|_{x=a_j}, \quad P_{i,j} = P_{i,j+1}, \quad x = a_j, \tag{22b}$$

$$D_{O_j} \frac{\partial O_j}{\partial x}\bigg|_{x=a_j} = D_{O_{j+1}} \frac{\partial O_{j+1}}{\partial x}\bigg|_{x=a_j}, \quad O_j = O_{j+1}, \quad x = a_j, \tag{22c}$$

where $i = 1, 2, \quad j = 1, 2.$

3.4 Response of the biosensor

The measured current is accepted as a response of an amperometric biosensor in a physical experiment. The current $I(t)$ depends upon the fluxes of the hexacyanoferrate(III) and mediator at the electrode surface,

$$I(t) = n_e F A \left(D_{P_{1,1}} \frac{\partial P_{1,1}}{\partial x}\bigg|_{x=0} + D_{P_{2,1}} \frac{\partial P_{2,1}}{\partial x}\bigg|_{x=0} \right), \tag{23}$$

where n_e is a number of electrons involved in the electrochemical reaction, F is Faraday's constant and A stands for the geometrical surface of the electrode.

We assume that the system (13)–(22) approaches a steady state as $t \to \infty$,

$$I_\infty = \lim_{t \to \infty} I(t), \tag{24}$$

where I_∞ is the steady state current.

4 Digital simulation

Because of non-linearity of the problem, no analytical solution is possible [30]. Hence the numerical simulation was employed. We applied a uniform discrete grid to simulate the biosensor using explicit finite difference method [24,32]. The program was implemented in Java programming language [34].

We assume the biosensor response I_R calculated at the moment T_R as the steady state response,

$$I_R = I(T_R) \approx I_\infty, \quad T_R = \min_{j>0, I_j>0} \left\{ \tau_j : \frac{I_j - I_{j-1}}{I_j} < \varepsilon \right\}, \quad \tau_j = \tau j, \tag{25}$$

where τ stands for the size of time step, $I_j = I(\tau_j)$. We used $\varepsilon = 10^{-3}$ for the calculations.

Table 1 Simulation parameters

Parameter	Value	Reference
a_1	$100\,\mu m$	[25]
a_2	$18.7\,\mu m$	[25]
a_3	$64.2\,\mu m$	[35]
k_1	$2.44\,\mu M^{-1}\,s^{-1}$	[15]
k_2	$0.26\,\mu M^{-1}\,s^{-1}$	[25]
k_3	$18\,\mu M^{-1}\,s^{-1}$	[25]
k_4	$330\,\mu M^{-1}\,s^{-1}$	[36]
E_0	$2.76\,\mu M$	[25]
$S_{1,0}$	$28\,\mu M$	[25]
$S_{2,0}$	$11\,\mu M$	[25]
O_0	$253\,\mu M$	[25]
$D_{S_{1,1}}, D_{S_{2,1}}, D_{P_{1,1}}, D_{P_{2,1}}$	$3.2 \times 10^{-10} m^2\,s^{-1}$	[37]
$D_{S_{1,2}}, D_{S_{2,2}}, D_{P_{1,2}}, D_{P_{2,2}}$	$5.6 \times 10^{-11} m^2\,s^{-1}$	[37]
$D_{S_{1,3}}, D_{S_{2,3}}, D_{P_{1,3}}, D_{P_{2,3}}$	$6.3 \times 10^{-10} m^2\,s^{-1}$	[37]
D_{O_1}	$2.01 \times 10^{-9} m^2\,s^{-1}$	[38]
D_{O_2}	$2.01 \times 10^{-9} m^2\,s^{-1}$	[38]
D_{O_3}	$2.01 \times 10^{-9} m^2\,s^{-1}$	[38]
$D_{E_{red,1}}, D_{E_{ox,1}}$	$3.6 \times 10^{-11} m^2\,s^{-1}$	[39]
n_e	1	[25]
A	$7 \times 10^{-6} m^2$	[25]

The values and references of the model parameters employed in the numerical experiments are summarized in Table 1.

5 Results and discussion

The behaviour of the laccase-based biosensor response was investigated by using computer simulation. By changing input parameters the biosensor action was analysed with a special emphasis to the influence of the species concentrations on the synergy of the simultaneous substrates conversion. The simulation was performed at wide ranges of the parameter values.

Figure 3 shows the steady-state profiles of the concentrations simulated at values given in Table 1. As expected, the concentrations of S_1 and S_2 are lower than the concentrations of P_1 and P_2 due to the enzymatic conversion of the substrates to the products. In the outer part of the enzyme layer, the concentrations are constant and they change gradually in the dialysis membrane and the diffusion layer. In the close proximity to the electrode, the increase of S_1 and the concomitant decrease of P_1 are observed due to the electrochemical reaction (11). A similar but relatively smaller change is followed by S_2 and P_2 which was probably caused by the reaction (12).

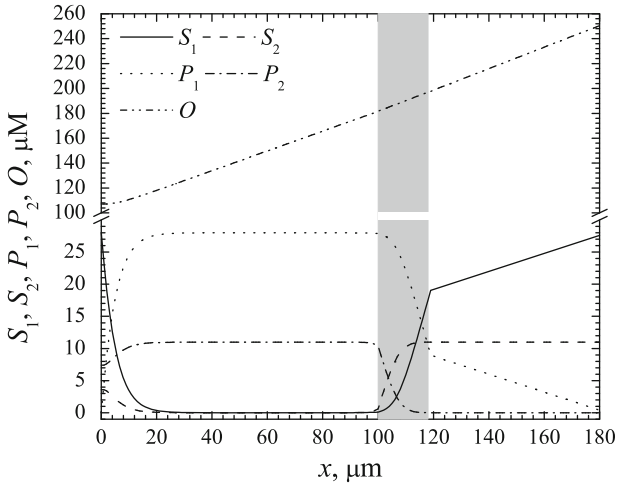

Fig. 3 The steady state concentration profiles of the ferrocyanide (S_1), mediator (S_2), ferricyanide (P_1), oxidased mediator (P_2) and oxygen (O) in the enzyme layer ($0 < x < 100\,\mu$m), dialysis membrane ($100 < x < 118.7\,\mu$m) and the diffusion layer ($118.7 < x < 182.9\,\mu$m). The grey zone represents the dialysis membrane. Values of the model parameters are given in Table 1

To see the effect of the mediator (substrate S_2) on the biosensor response, two different experiments were simulated. The simulated biosensor currents are depicted in Fig. 4. In the initial stage of both simulated experiments, only the first substrate S_1 ($S_{1,0} = 28\,\mu$M) was infused into the buffer solution. When the system has reached the steady state ($t = 800$ s), an additional substrate was infused. In the first case of the biosensor operation (curve 1), the mediator (second substrate, $S_{2,0} = 11\,\mu$M) was infused keeping the concentration of S_1 unchanged, while in the second case (curve 2) an additional amount of S_1 was infused keeping the zero concentration of S_2. Finally, the total concentration of the substrates was the same ($S_{1,0} + S_{2,0} = 39\,\mu$M) in both cases. As one case see in Fig. 4 that the addition of the hexacyanoferrate(II) (substrate S_1, curve 2) increases the bioelectrode current, which after ca. 200 s reaches the steady-state. However, the addition of the mediator (substrate S_2, curve 1) causes a supplementary increase of the bioelectrode response over that which is attained with equal amount of S_1.

The addition of the mediator cases additional increase of the bioelectrode response (Fig. 4). To investigate this effect in details, the bioelectrode responses were simulated at a wide range of the mediator concentrations. Figure 5 shows the dependence of the steady state bioelectrode response I_R on the concentration $S_{2,0}$ of the mediator at three enzyme concentrations E_0. The increase of the current notably depends on the mediator concentration. The dependence of I_R on $S_{2,0}$ is practically linear up to $10\,\mu$M. At higher concentrations of the mediator, the dependence of the current on the mediator concentration shows a saturation character. Very similar dependence of the response on the mediator concentration was observed in real experiments [25]. In [25] the observation was made that the bioelectrode sensitivity was dependent on

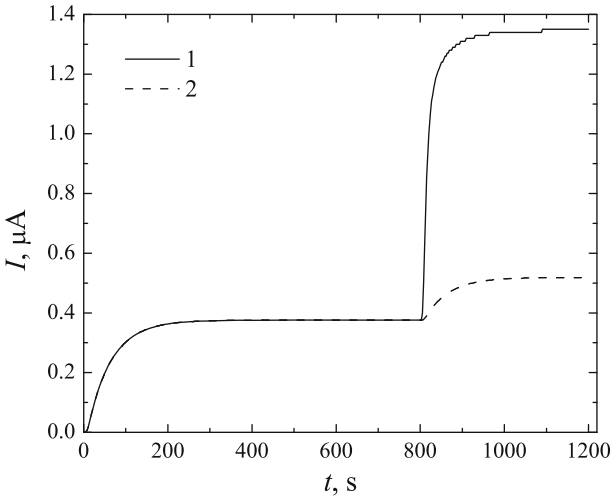

Fig. 4 The change of the laccase-based biosensor current $I(t)$ in two operation cases: (1) the concentration $S_{2,0}$ of the mediator was set to 11 μM at time $t = 800$ s, (2) in absence of mediator ($S_{2,0} = 0$) the concentration $S_{1,0}$ of the ferrocyanide was increased to 39 μM at time $t = 800$ s. The other parameters are the same as in Fig. 3

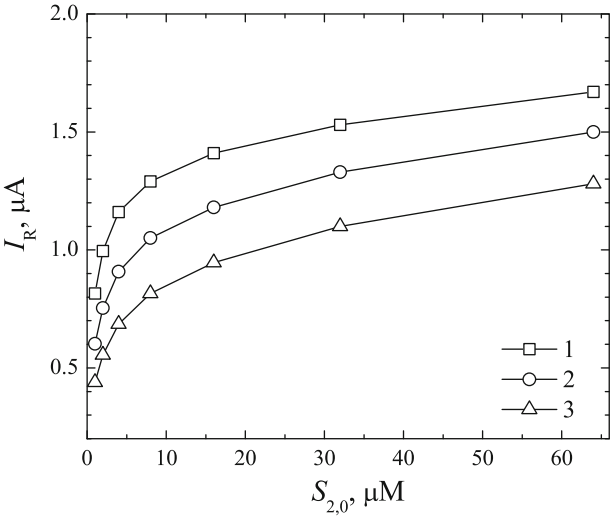

Fig. 5 The dependence of steady state bioelectrode response I_R on the concentration $S_{2,0}$ of the mediator at three enzyme concentrations E_0: 2.76 (1), 1.38 (2), 0.69 (3) μM. The other parameters are listed in Table 1

immobilized laccase concentration. Contradictory results were obtained by using the modelling as sensitivity was nearly unchanged in the range of E_0 from 0.69 to 2.76 μM.

Figure 6 presents the dependence of the bioelectrode response on the concentration $S_{1,0}$ of ferrocyanide (S_1) and time (t). As it is apparent from Fig. 6, the increase of the current upon the addition of the mediator also depends on the concentration $S_{1,0}$

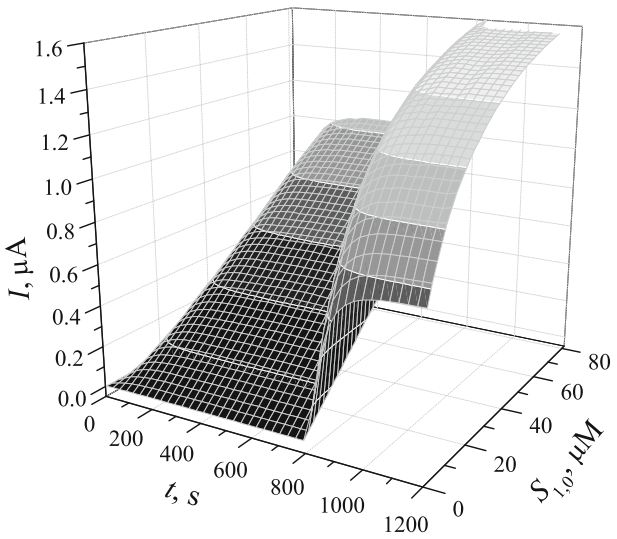

Fig. 6 The dynamics of the bioelectrode response at different concentrations $S_{1,0}$ of ferrocyanide. The other parameters are listed in Table 1

of ferrocyanide. With the higher amount of $S_{1,0}$, a relatively smaller increase of the current is obtained. This can be explained by the competitive action of S_1 and S_2. S_1 competes with S_2 for the binding to the active site of laccase, and, at the high concentrations $S_{1,0}$ of ferrocyanide, there is almost none of P_2, which participates in the synergistic reaction, produced.

In order to estimate the limits of synergistic effect it is useful to introduce the difference I_S,

$$I_S = I_R - I_{0R}, \tag{26}$$

where I_{0R} stands for the steady state current before the addition of the mediator [25]. I_S is the the current calculated by withdrawing from the overall bioelectrode current the bioelectrode current in the presence of ferrocyanide at zero mediator concentration. The difference I_S between the steady state currents I_R and I_{0R} can be called as the synergistic current [25].

Figure 7 shows the dependence of the synergistic current I_S on the enzyme concentration E_0. The source currents I_R and I_{0R} are also depicted in Fig. 7. As one can see in Fig. 7 the synergistic current I_S is a non-monotonous function of E_0. It shows that the synergistic current reaches a maximum at $E_0 = 5\,\mu\text{M}$. Below that value, small amount of product P_2 is produced for the synergetic reaction to occur. Above the peak value, most of S_1 is consumed in reaction (8) hindering the synergetic reaction.

Figure 8 shows the dependence of the synergistic current I_S on the concentration $S_{1,0}$ of the ferrocyanide (substrate S_1). This dependence can be explained similarly as the dependence of I_S on the enzyme concentration E_0. At very high concentrations

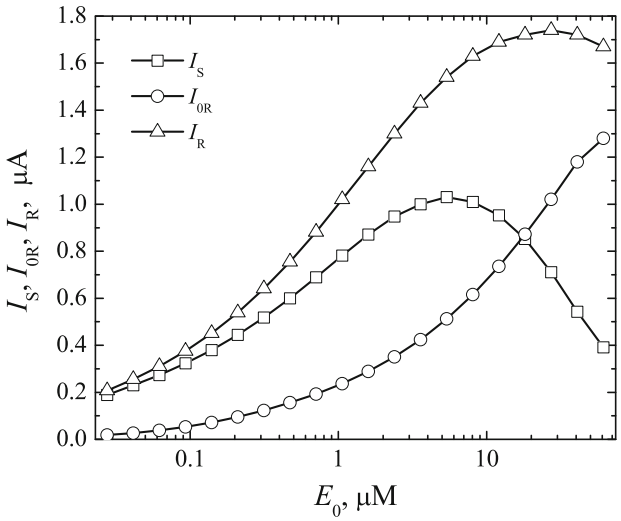

Fig. 7 The steady state bioelectrode responses I_R and I_{0R} as well as the synergistic current I_S versus the enzyme concentration E_0. The other parameters are listed in Table 1

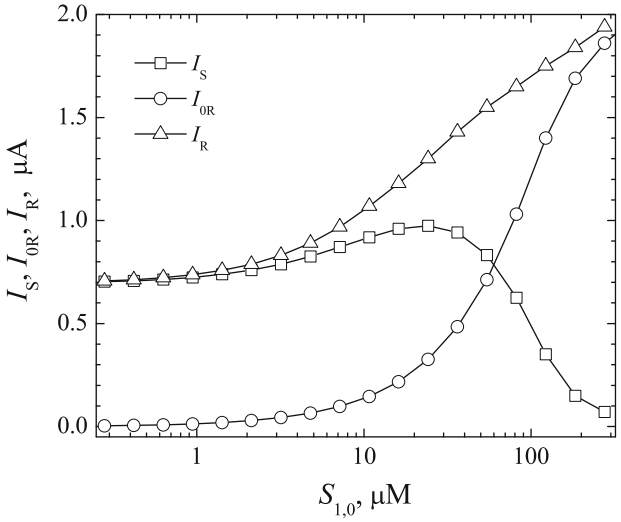

Fig. 8 The dependences of the steady state bioelectrode responses I_R and I_{0R} as well as the synergistic current I_S on the substrate concentration $S_{1,0}$ at values of the model parameters given in Table 1

$S_{1,0}$ of the substrate S_1, the enzyme is mostly involved in reaction (8) and this slows down the production of the product P_2 which is necessary for the synergetic reaction.

6 Conclusions

The developed mathematical model (13)–(23) can be successfully used to simulate the behavior of the laccase-based biosensor utilising simultaneous substrates conversion (Fig. 1).

The synergistic current I_S is a non-monotonous function of the enzyme concentration E_0 (Fig. 7) as well as of the substrate concentration $S_{1,0}$ (Fig. 8). The limits of synergistic effect were estimated with the maximum synergistic current I_S obtained at $E_0 = 5\,\mu\text{M}$ and $S_{1,0} = 12\,\mu\text{M}$. Taken together, these results confirm the synergistic effect in the laccase biosensor [25].

The synergistic effect of the laccase-based biosensors can be increased by selecting an appropriate concentration of the enzyme as well as values of some other model parameters. The computational simulation of the biosensor response can be used as a tool in design of novel highly sensitive laccase-based biosensors.

To prove conclusions made the experiments are running using laccase-based biosensors with different geometry and catalytical parameters.

Acknowledgments This research was funded by the European Social Fund under Measure VP1-3.1-SMM-07-K "Support to Research of Scientists and Other Researchers (Global Grant)", Project "Developing computational techniques, algorithms and tools for efficient simulation and optimization of biosensors of complex geometry".

References

1. F. Scheller, F. Schubert, *Biosensors* (Elsevier, Amsterdam, 1992)
2. A.P.F. Turner, I. Karube, G.S. Wilson, *Biosensors: Fundamentals and Applications* (Oxford University Press, Oxford, 1987)
3. N.J. Ronkainen, H.B. Halsall, W.R. Heineman, Chem. Soc. Rev. **39**(5), 1747 (2010)
4. U. Wollenberger, F. Lisdat, F.W. Scheller, *Frontiers in Biosensorics 2, Practical Applications* (Birkhauser, Basel, 1997)
5. B.D. Malhotra, A. Chaubey, Sens. Actuators **B91**(1–3), 117 (2003). doi:10.1016/S0925-4005(03)00075-3
6. S. Viswanathan, H. Radecka, J. Radecki, Monatshefte Fur Chemie **140**(8), 891 (2009)
7. D. Yu, B. Blankert, J.C. Viré, J.M. Kauffmann, Anal. Lett. **38**(11), 1687 (2005). doi:10.1080/00032710500205659
8. A. Chaubey, B.D. Malhotra, Biosensors and Bioelectronics **17**(6–7), 441 (2002)
9. A. Cornish-Bowden, *Fundamentals of Enzyme Kinetics* (Portland Press, London, 2004)
10. F. Barrire, P. Kavanagh, D. Leech, Electrochimica Acta **51**(24), 5187 (2006)
11. M. Cooney, V. Svoboda, C. Lau, G. Martina, S.D. Minteer, Energy Environ. Sci. **1**, 320 (2008)
12. R.S. Freire, C.A. Pessoa, L.D. Mello, L.T. Kubota, J. Brazilian Chem. Soc. **14**(2), 230 (2003)
13. O. Morozova, G. Shumakovich, M.A. Gorbacheva, S.V. Shleev, A.I. Yaropolov, Biochemistry (Moscow) **72**(10), 1136 (2007)
14. K. Servat, S. Tingry, L. Brunel, S. Querelle, M. Cretin, C. Innocent, C. Jolivalt, M. Rolland, J. Appl. Electrochem. **37**(1), 121 (2007)
15. L. Tetianec, J. Kulys, Central European J. Biology **4**(1), 62 (2009)
16. J. Kulys, R. Vidziunaite, Biosensors and Bioelectronics **18**(2–3), 319 (2003)
17. J. Kulys, Ž. Dapkūnas, Nonlinear Anal. Model. Control **12**(4), 495 (2007)
18. C. Amatore, A. Oleinick, I. Svir, N. da Mota, L. Thouin, Nonlinear Anal. Model. Contr **11**(4), 345 (2006)
19. I. Stamatin, C. Berlic, A. Vaseashta, Thin Solid Films **495**(1–2), 312 (2006). doi:10.1016/j.tsf.2005.08.299
20. L.D. Mell, T. Maloy, Anal. Chem. **47**(2), 299 (1975)

21. J. Kulys, Anal. Lett. **14**(B6), 377 (1981)
22. P.N. Bartlett, R.G. Whitaker, J. Electroanal. Chem. **224**(1–2), 27 (1987)
23. T. Schulmeister, D. Pfeiffer, Biosensors and Bioelectronics **8**(2), 75 (1993)
24. R. Baronas, F. Ivanauskas, J. Kulys, *Mathematical Modeling of Biosensors, Springer Series on Chemical Sensors and Biosensors, vol 9* (Springer, Dordrecht, 2010)
25. J. Kulys, R. Vidziunaite, Electroanalysis **21**(20), 2228 (2009)
26. M.E.G. Lyons, J. Murphy, S. Rebouillat, J. Solid State Electrochem. **4**, 458 (2000)
27. P.N. Bartlett, K.F.E. Pratt, J. Electroanal. Chem. **397**(1–2), 61 (1995)
28. R. Baronas, F. Ivanauskas, J. Kulys, J. Math. Chem. **35**(3), 199 (2004)
29. M.E.G. Lyons, Sensors **6**(12), 1765 (2006)
30. D. Britz, *Digital Simulation in Electrochemistry, Lecture Notes in Physics, 3rd edn. vol 666* (Springer, Berlin/Heidelberg, 2005). doi:10.1007/b97996
31. A. Meena, A. Eswari, L. Rajendran, J. Math. Chem. **48**(2), 179 (2010)
32. A.A. Samarskii, *The Theory of Difference Schemes* (Marcel Dekker, New York-Basel, 2001)
33. S. Whitaker, *The Method of Volume Averaging, Theory and Applications of Transport in Porous Media, vol 13* (Kluwer Academic Publishers, Boston, 1999)
34. J.E. Moreira, S.P. Midkiff, M. Gupta, P.V. Artigas, M. Snir, R.D. Lawrence, IBM Syst. J. **39**(6), 21 (2000)
35. J. Kulys, V. Razumas, *Bioamperometry* (Mokslas, Vilnius, 1986)
36. J. Kulys, L. Tetianec, I. Bratkovskaja, Biotechnology J. **5**, 822 (2010)
37. D.A. Gough, J.K. Leypoldt, Anal. Chem. **51**(3), 439 (1979)
38. R. Bird, W. Stewart, E. Lightfoot, *Transport Phenomena* (Wiley, NY, 1960)
39. S. Shleev, A. Christenson, V. Serezhenkov, D. Burbaev, A. Yaropolov, L. Gorton, T. Ruzgas, Biochemical J. **385**(3), 745 (2005)